3D RTM angle gathers using an inverse scattering imaging condition

Sverre Brandsberg-Dahl, Nizar Chemingui, Dan Whitmore, Sean Crawley, Elena Klochikhina and Alejandro Valenciano. PGS

Summary

Reverse-time migration applied to shot gathers, has typically outputs stacked images. This does not allow for the use of the multi-dimensionality of the data after imaging. For todays wide- and full-azimuth acquisitions this imposes a strong limitation on our ability to fully utilize the data quality and subsurface illumination such surveys offer.

Here, we present an implementation of reverse-time migration that allows for the output of azimuth-sectored angle gathers in all CDP locations in the image space. These 3D angle-gathers are virtually artifact free as we use an inverse scattering imaging condition that effectively removes the backscatter noise during the imaging step. With access to angle gathers for the whole image volume, we can deploy conventional strategies of muting, editing, noise suppression and residual corrections before stacking, leading to much improved images in both extra-salt and complex sub-salt regions.

Introduction

In its simplest form, correlation based RTM imaging conditions generate significant low wavenumber artifacts. These artifacts are most often generated by the backscattered and turning waves in the modeling process, which causes the incident and reflected wavefields to be in phase at locations that are not the reflection points. Reducing these artifacts is often achieved by post processing the image or modifying the imaging conditions to reduce the artifacts in the first place -- or some combination of both.

The classic way to produce a stacked, migrated image in RTM is via the cross correlation imaging condition (Claerbout, 1985):

$$I(\bar{x}) = \sum_{x_s} \sum_{x_g} \int_0^{t\max} p_s(\bar{x},t;\vec{x}_s)\, p_g(\bar{x},T-t;\vec{x}_g)\, dt \qquad (1)$$

where the image I is the stack over all shots, receivers, and times, of the cross correlation of the forward-modeled source wavefield p_S and the back-propagated receiver wavefield p_g.

Numerous methods have been formulated to extend I to migrated prestack data in the form of angle-domain common image gathers (ADCIGS), for example Dickens and Winbow (2011). In many cases, the migration algorithm is modified to produce some form of offset-domain common image gathers (ODCIGS), which are later converted to angle.

Rickett and Sava (2002) converted horizontal source-receiver offset in the subsurface to reflection angle. Subsurface offset gathers come from adding x and y correlation lags to the image in equation (1). After forming the image gathers, we can perform post processing to remove artifacts and to improve the image in general.

However, the gathers still tend to suffer from artifacts caused by backscattered energy. Recent works by multiple authors have focused on methods that use imaging conditions that use the direction of the propagating wavefields directly in the imaging kernel to reduce the generation of these artifacts (Whitmore et al. 2012). Below we will outline how an imaging condition based on inverse scattering theory (Stolk et al. 2009) can be implemented to allow for efficient generation of 3D angle gathers that are virtually free from artifacts caused by backscattered energy.

Method

Far field directions (ray parameters) of the propagating source and receiver wavefields are approximated by:

$$\mathbf{p}_S \cong \frac{\nabla S(\bar{x},t)}{\dfrac{\partial S(\bar{x},t)}{\partial t}} \qquad \mathbf{p}_R \cong \frac{\nabla R(\bar{x},t)}{\dfrac{\partial R(\bar{x},t)}{\partial t}} \qquad (2)$$

The approximate direction angles for the propagating wavefields can also be computed from the ray parameters. The subsurface reflection angle information can be computed from the above quantities as follows

$$\cos(\mathbf{p}_S,\mathbf{p}_r) \cong \frac{\mathbf{p}_S \bullet \mathbf{p}_R}{|\mathbf{p}_S||\mathbf{p}_R|} \qquad |\mathbf{p}_S||\mathbf{p}_R| = \frac{1}{V^2} \qquad (3)$$

providing us access to the necessary information for binning the data into angle bins. Note that the cosine of the opening angle is directly correlated to locations where the wavefields are in phase.

Azimuth, can be computed similarly, and tracked as an additional axis in the output gathers. In the example presented below, we measure the azimuth between the source direction vector and the survey inline direction, but other definitions can be accommodated as well, as this all is related to simple vector calculus.

Figure 1 shows snapshots for the source and receiver wavefields and the source propagation angles and cosine of opening angle at a single time.

The general inverse scattering condition is given in equation (4),

$$I(x) = \frac{1}{2A(x)}\left[\int W_1(x,t)\nabla\Psi_S(x,t)\cdot\nabla\Psi_R(x,T-t) + W_2(x,t)\frac{1}{V^2(x)}\frac{\partial\Psi_S(x,t)}{\partial t}\frac{\partial\Psi_R(x,T-t)}{\partial t}dt\right] \quad (4)$$

where Ψ_S and Ψ_R are the frequency scaled versions of the source S(**x**,t) and R(**x**,t) respectively:

$$\Psi_S(x,t) = \frac{1}{2\pi}\int e^{i\omega t} i\omega^{-\alpha}\hat{S}(\mathbf{x},\omega)$$

$$\Psi_R(x,t) = \frac{1}{2\pi}\int e^{i\omega t}\omega^{-1}\hat{R}(\mathbf{x},\omega)$$

With the addition of appropriately computed weights, this general imaging condition attenuates the low wavenumber RTM artifacts occurring in more complex media, including the case of turning waves. In equation (4) the weights are written as both a function of space and time. However, these weights can also be chosen to be constant and equal (equivalent to Stolk, et. al.), a function of space only (to be applied after the sum over shots) or as a function of angles (to be applied to angle volumes or gathers).

Using the above imaging condition and with a angle binning scheme based on the wavefront normal, we have implemented a framework for RTM that allows for efficient output of 3D angle gathers at all CDP locations. This enables us to perform a range of processing steps on the data, post-migration, but pre stack.

2D example, angle gathers

The first example is a real data case from offshore Africa. In this case, angle gathers from a TTI RTM image were generated. The inverse scattering imaging condition was applied to each angle separately, and then the data was summed over angle. For comparison, the angle gathers and stacks with and without application of the inverse scattering imaging condition are shown in Figure 2. Note the reduction in RTM artifacts for both the angle gathers and the final stacks.

These angle gathers have subsequently been used for velocity model building with tomography (Zhou et al. 2012).

Field data example with 3D angle gathers

Our second example is based on a wide azimuth (WAZ) dataset from the Gulf of Mexico. This data was processed through a TTI RTM flow, where we output 3D angle-gathers at every CDP in the image volume. The effect of the inverse scattering imaging condition is illustrated in Figure 3, where the artifacts associated with backscattered energy are clearly visible on the image generated with a standard correlation imaging condition. Using the same data and TTI velocity model, but with our new imaging condition, we produce an image virtually free of these artifacts.

With a complete set of 3D (azimuth and opening angle) gathers, we are able to apply a range of post-migration processing and conditioning before stack. In addition to residual moveout corrections, we are able to filter, mute and selectively stack the image gathers. Figure 4 shows a set of angle gathers after selective/smart stacking of the azimuth sectors and application of a 3D spatially variable mute. The mute is driven by the salt model. The bottom part of the figure compares a sub-salt depth slice at 8km for a "raw" stack and a stack of the muted and processed angle gathers. The subsalt image is much improved, and the structure of the sub-salt mini basin is now clearly visible.

Conclusions

Reverse time migration (RTM) imaging can have significant artifacts which are generated by backscattered and turning waves, where the source and receiver wavefields are in phase. This paper introduces an inverse scattering based imaging condition that in our implementation allows for efficient output of 3D angle gathers (azimuth and opening angle) at every CDP location in the image. The method is based on an imaging kernel that is the weighted combination of two separate imaging kernels – the time derivative product and the gradient dot product of the source and receiver wavefields respectively. We show applications of this method to two field data examples. A 2D case from West Africa and a 3D wide azimuth example from the Gulf of Mexico.

Acknowledgements

The authors wish to thank PGS for permission to publish this work.

3D angle gathers using inverse scattering imaging condition

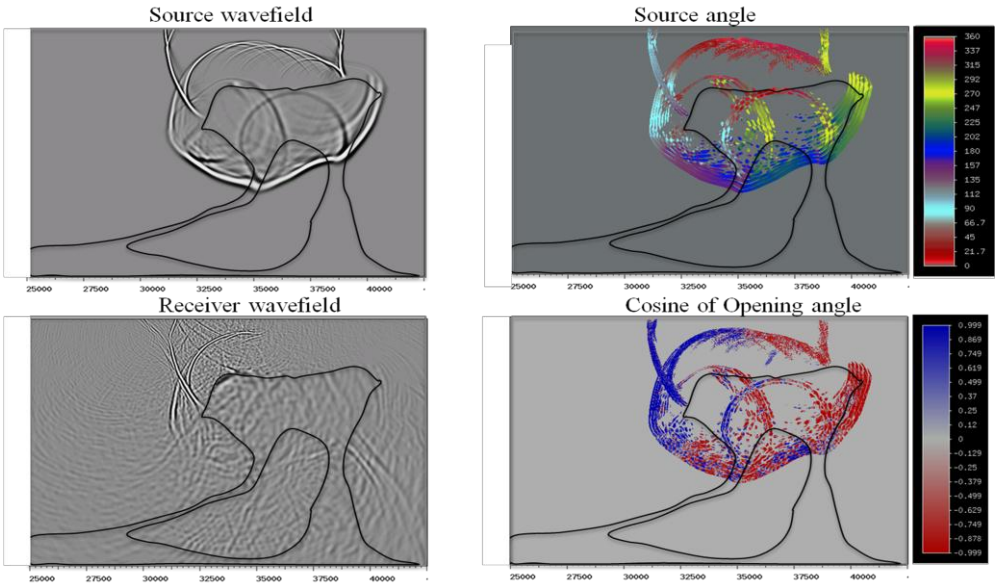

Figure 1: Wavefield snapshots: Source wavefield, receiver wavefield, source angle (relative to x axis) and cosine of opening angle. Note that the source and receiver wavefields are in phase where the cosine of the opening angle is approximately one (blue color)

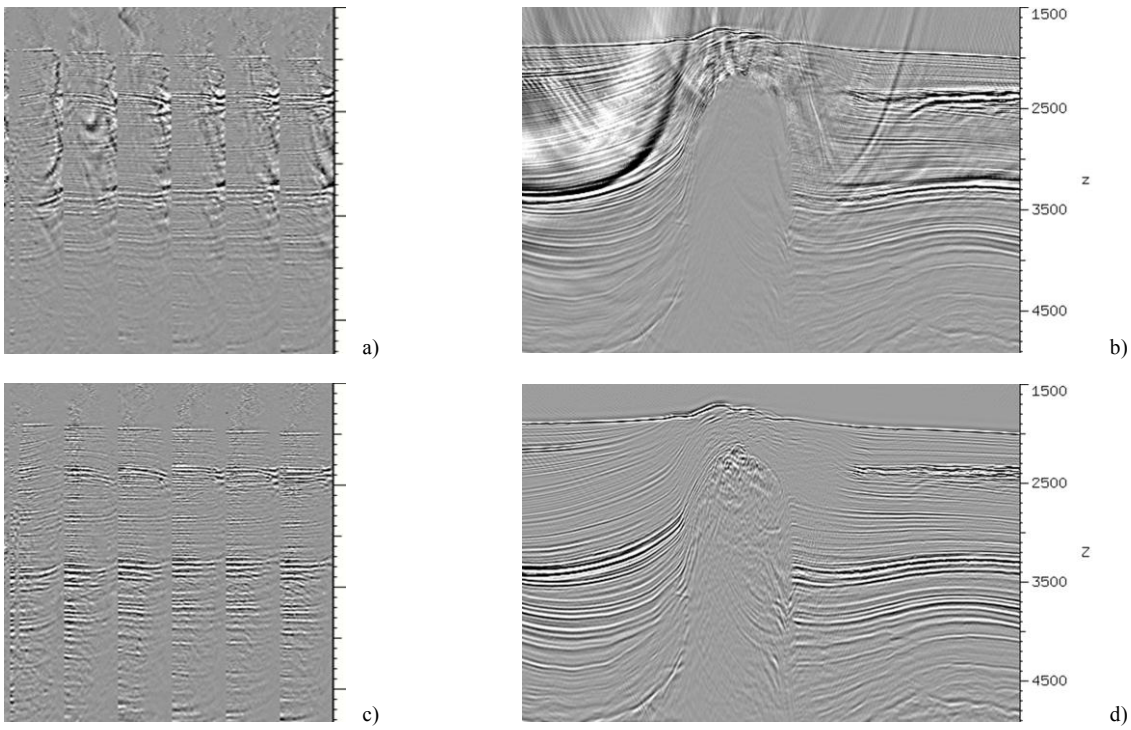

Figure 2: Angle gathers and stacks for correlation and general inverse scattering imaging conditions. The two top images a) and b) show the angle gathers and stack from standard correlation imaging condition, and the bottom two images c) and d), show the same data after application of our inverse scattering imaging condition.

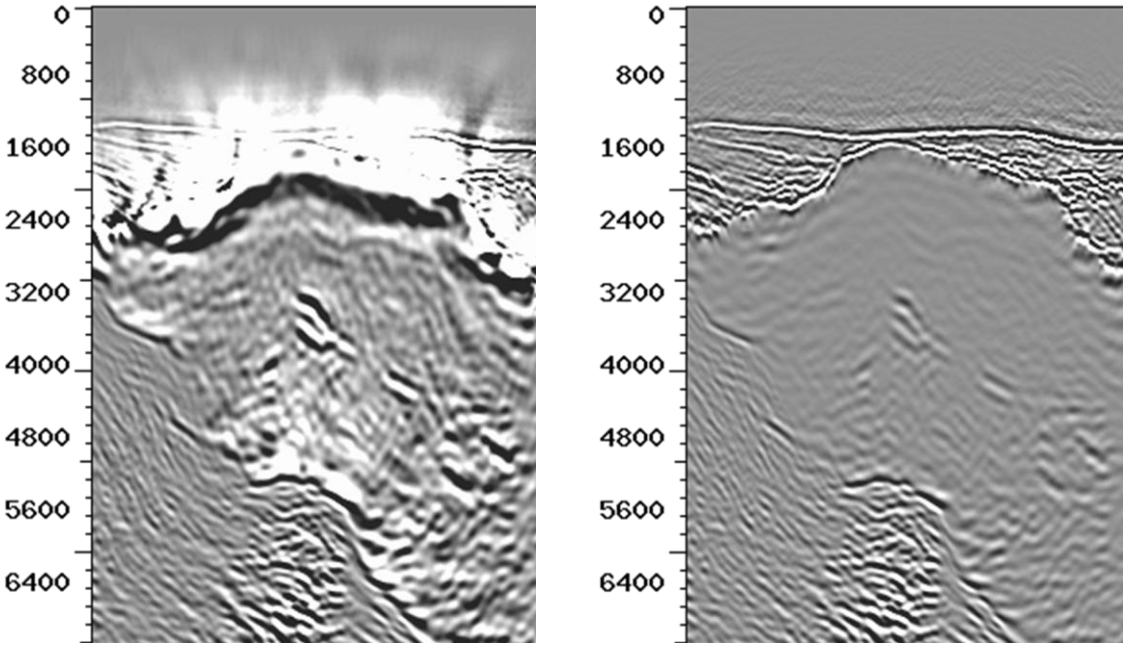

Figure 3: Comparison of full salt model TTI RTM of a Gulf of Mexico WAZ dataset using correlation imaging condition (left) and our inverse scattering imaging condition (right). Note the very compact wavelet achieved on top salt, as well as the overall clean up of artifacts associated with backscattered energy.

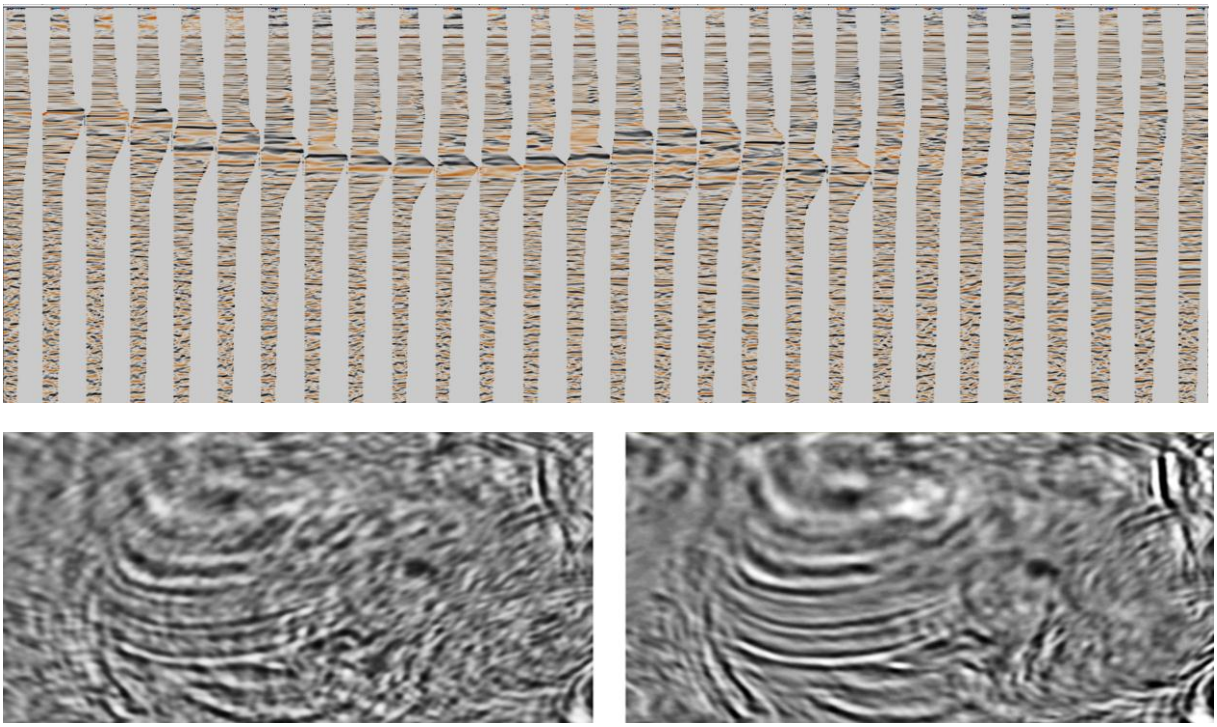

Figure 4: The top figure shows the angle gathers after the application of the spatially variable mute. The bottom two images show sub-salt depth slices at 8km. The left image is generated without muting and processing of the 3D angle gathers and is impacted by incoherent energy and conflicting events in the subsalt mini-basin. The picture on the right shows the cleanup achieved after muting and processing of angle gathers.

http://dx.doi.org/10.1190/segam2013-1402.1

EDITED REFERENCES

Note: This reference list is a copy-edited version of the reference list submitted by the author. Reference lists for the 2013 SEG Technical Program Expanded Abstracts have been copy edited so that references provided with the online metadata for each paper will achieve a high degree of linking to cited sources that appear on the Web.

REFERENCES

Stolk, C. C., M. V. De Hoop, and T. Op't Root, 2009, Linearized inverse scattering based on seismic reverse-time migration: Proceedings of the Project Review, Geo-Mathematical Imaging Group (Purdue University, West Lafayette IN), Vol. 1 pp. 91-108 and Journal de Mathématiques Pures et Appliquées, 2011.

Billette, F., and S. Brandsberg-Dahl, 2005, The 2004 BP velocity benchmark: 67th Annual Conference and Exhibition, EAGE, Extended Abstracts, B035.

Claerbout, J. F., 1985, Imaging the earth's interior: Blackwell Science Inc.

Dickens, T. A., and G. A. Winbow, 2011, RTM angle gathers using Poynting vectors: 81st Annual International Meeting, SEG, Expanded Abstracts, 3109–3113.

Rickett, J. E., and P. C. Sava, 2002, Offset and angle-domain common image-point gathers for shot-profile migration: Geophysics, **67**, 883–889, http://dx.doi.org/10.1190/1.1484531.

Whitmore, N. D. and S. Crawley, 2012, Applications of RTM inverse scattering imaging conditions: 82nd Annual International Meeting, SEG, Expanded Abstracts, http://dx.doi.org/10.1190/segam2012-0779.1.

Zhou, C., N. D. Whitmore, and Sverre Brandsberg-Dahl, 2012, Multiparameter joint tomography model building with angle gathers: 82nd Annual International Meeting, SEG, Expanded Abstracts.